

Identifying Learning in a Visuomotor Skill

Journal:	<i>Transactions on Biomedical Engineering</i>
Manuscript ID:	TBME-00100-2011
Manuscript Type:	Paper
Date Submitted by the Author:	03-Feb-2011
Complete List of Authors:	Abdur-Rahim, Jamilah; University of California, Santa Barbara, Dept. Mechanical Engineering Petzold, Linda; University of California, Santa Barbara, Dept. Computer Science, Dept. Mechanical Engineering Grafton, Scott; University of California, Santa Barbara, Dept. Psychology Doyle, Frank; University of California, Santa Barbara, Dept. Chemical Engineering
TIPS:	System identification, State space methods, Output feedback, Cognitive science

SCHOLARONE™
Manuscripts

Only

Identifying Learning in a Visuomotor Skill

Jamilah A. Abdur-Rahim, *Student Member, IEEE*, Linda R. Petzold,

Scott T. Grafton, and Francis J. Doyle III, *Fellow, IEEE*,

Abstract—We develop a framework for model selection, using structured and unstructured linear time invariant control models, to describe human motor behavior for individual trials of a compensatory tracking experiment. We develop new metrics for quantifying performance and learning across trials using state space model parameters. Changes in metric parameter values obtained from the control model estimates are used to characterize learning. Classification of participants based on error performance provides a means to test how it relates to a set of model parameters that describe both performance and learning. We highlight the many benefits of using unstructured models, including the ability to quantify the evolution of the human control policy across trials.

Index Terms—System identification, State space methods, Output feedback, Cognitive science.

I. INTRODUCTION

Motor learning is a change in capacity to generate behavior, and quantified in visuomotor experiments as a change in performance via reduction of error over training. Both compensatory and pursuit tracking experiments are used to demonstrate motor learning because: the movement is continuous, the input signal can be predictable or irregular, and the cursor movement can be determined by position, velocity, or acceleration of the controller [1]. Previous studies described visually guided control as a feedback controller [2], [3]. These models used control policy parameters, which are directly related to the task, to describe performance. Learning was described in terms of simple error reduction. However, error alone does not yield insight into the intrinsic system dynamics.

Modeling motor control and learning with performance data is challenging because the model structure is intrinsically unknown and must be inferred from the measured behavior. Thus, it is necessary to make assumptions about putative control models. The recent literature has described performance and learning in a two-step process: 1) identification of the control policy with direct labeling of feedforward and feedback parameters and 2) iterative estimation the states and parameters of the control policy model using Kalman filtering based analysis [4], [5]. Motor performance is also described in the context of optimal control theory, showing that humans optimize performance by minimizing a cost function that has linear quadratic behavior. This approach can explain variances in response behavior [6], [7]. Approaches that incorporate a control policy with either Kalman filtering or optimal control

analysis are potentially problematic because the control policy for human motor performance and the model for human motor learning are unknown. Thus, many simulations use the simplest possible task-related control policy and learning model, such as a PD controller. Despite these limitations, recently proposed models of motor learning have captured the effects of learning through improved predictive capability of performance [5]. Alternatively, subspace identification makes very few assumptions about model structure and has previously been used to verify the quality of fit for competing performance models (optimal, nonlinear, etc.), to estimate state space parameters that relate directly to physical experimental quantities such as error and change in error, and to estimate performance models for individual subjects for trials pooled across time [7], [8], [9].

At the current time, models of human learning are lacking in several important aspects. Notably, they exhibit residual errors in predicting participant performance. Furthermore, many of the proposed model structures do not change within trials or from trial-to-trial, and few capture individual differences from participant-to-participant. Most importantly, there does not exist a unifying framework that allows for the comparison of performance, learning, and predictive parameters of existing models. Accurate, simple, and easily customizable trial-by-trial models are needed in order to quantify the progression of learning and assist in the process of understanding what physical and/or behavioral parameters are important in terms of motor learning. There already exist tools to validate individual control models and determine how well they predict human data. For competing models, the question then arises how can one determine which model is best for describing human behavior, particularly when they exhibit similar fits to data.

In this paper, we present a framework that allows for the comparison of performance, learning, and predictive parameters for a set of control models expressed in the state space form and implemented across individual trials. Performance is identified by model prediction parameters, and learning is identified by model feedforward parameters. We compare three models within the developed framework: a third-order subspace model (SS3), an unconstrained-order subspace model (SSbest), and a third-order proportional derivative controller

J. A. Abdur-Rahim is in the Department of Mechanical Engineering, University of California, Santa Barbara, CA 93106-5070.
E-mail: jamilah@engineering.ucsb.edu.

L. R. Petzold is in the Departments of Computer Science and Mechanical Engineering, University of California, Santa Barbara, CA 93106-5070.
E-mail: petzold@cs.ucsb.edu.

S. T. Grafton is in the Department of Psychology, University of California, Santa Barbara, CA 93106-9660.
E-mail: grafton@psych.ucsb.edu.

F. J. Doyle III is in the Department of Chemical Engineering, University of California, Santa Barbara, CA 93106-5080.
E-mail: frank.doyle@icb.ucsb.edu.

(PD). The PD controller was a natural choice because it is the most widely employed approach for characterizing feedback control, and the proportional and derivative parameters are properties inherent to motor control. The Numerical Subspace State Space System Identification (N4SID) algorithm was used to model motor performance. We focus on data from a 1-dimensional visuomotor compensatory tracking task where the cursor movement is based on the velocity of the motor output [5]. In the experiment, described in more detail in Section II, the subject views a centered vertical stationary red bar and a vertical moving yellow bar that is perturbed by an external input signal. The task involves moving the yellow bar, by applying force to a fixed knob, so that it is centered and aligns with the red bar. The error in the experiment is then calculated using the Root Mean Square (RMS) measure. The experiment was originally designed to measure changes of tracking error when the input signal is repeated and sufficiently simple that it can be predicted after practice.

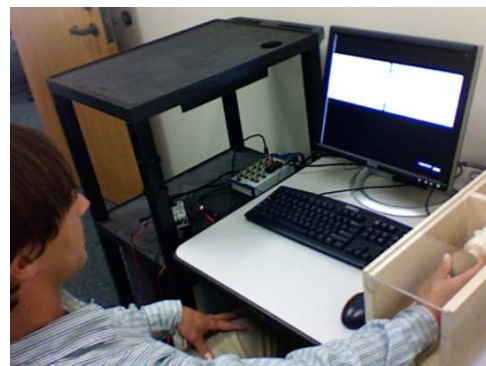
After model validation for each of the three models, we use the model prediction, feedback, and feedforward parameters to identify the best model that describes human motor behavior. Our approach provides a solution in terms of model selection based on the additional parameters (feedback, feedforward) to compare amongst competing models. Selection of the best model to represent human behavior is not solely based on model prediction, but on trends in the feedback and feedforward parameters that confirm or relate to existing human motor behavior attributes.

This paper is organized as follows. Section II (Methods) discusses the construction of the three models, experimental setup, and pre-modeling analysis. Section III (Results) presents the collected data in time and frequency domain and model comparisons for model performance, feedback, and feedforward. Section IV concludes with a discussion of how models compared with one another based on the framework.

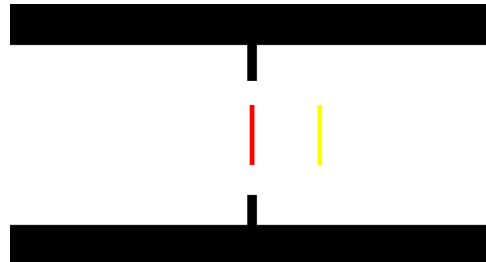
II. METHODS

A. Experimental Setup

We used data for nine right-handed adults from an experiment performed over a period of four days [5]. One subject was excluded because the data set was incomplete. The participants had normal corrected vision and learned a visuomotor compensatory tracking task driven by a pair of symmetric *arctan* input functions, one to the right and one to the left, which alternated from trial to trial. Participants viewed a computer screen similar to Figure 1(b), where a stationary vertical red bar that serves as the target bisects the white area of the screen. The knob controls the lateral position of a second, thick yellow vertical bar. The cursor has velocity control movement, thus the angular position of the knob translates into the velocity of the cursor on the screen. There were four runs each day, each of which consisted of 26 tracking task trials. Participants used their right hand to respond to 13 trials where the *arctan* input drove the cursor to the left, and 13 trials where the *arctan* input drove the cursor to right. Each run started with 30 seconds of rest, followed by 10 seconds for the tracking task trial alternating with 10



(a) Participant performing an identical visual motor compensatory task.



(b) Typical view of the computer screen during a tracking trial.

Fig. 1: Behavioral experimental set-up and a snapshot of the computer screen for a typical trial.

seconds of rest, and ending in 35 seconds of rest. The goal for each trial was to rotate the knob to keep the yellow bar from deviating from the red bar. All data was collected at a constant sampling rate of 0.0079 seconds for each data point.

B. Data preprocessing

Before models were constructed, the participants' performance and the input disturbance function were preprocessed using the same methodology used in [5]. That methodology included filtering (fifth-order Butterworth filter), calculation of velocity and acceleration, and removal of extreme outliers. Results for the left *arctan* input are shown to illustrate key results; the error reduction trend for the left and right *arctan* input were similar except that the total normalized average median error for the right *arctan* was 0.83, whereas the left *arctan* was 0.18. Figure 2 shows representative data for a left *arctan* input that corresponds to position control. The cursor started to the right of the center of the screen and slowly moved to the center. The middle subplot shows the numerical derivative of the top subplot, i.e., velocity control. The bottom subplot shows the numerical second derivative of the top subplot, i.e., acceleration control. A standard measure of participant performance in motor learning experiments is model error; the participants' error is a direct indicator for quantifying the amount of learning. The root mean squared error (RMSE) corresponding to position control was individually calculated for the eight participants as

$$\text{RMSE} = \sqrt{\frac{\sum_{i=1}^N e_i^2}{N}}. \quad (1)$$

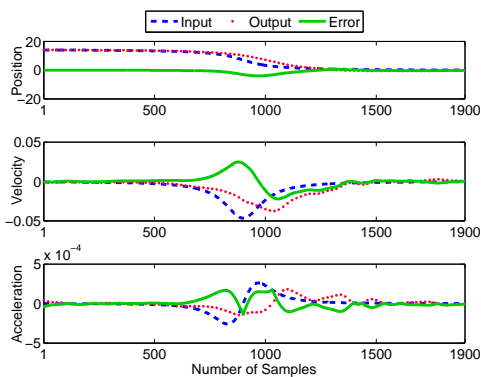
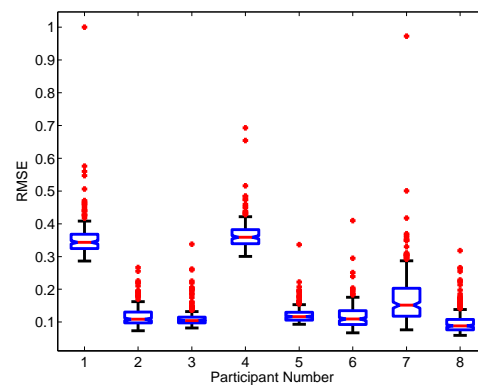


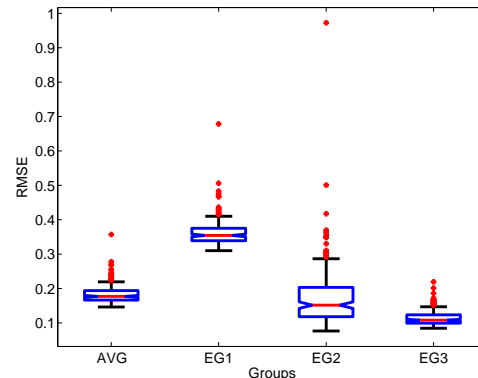
Fig. 2: The subplots show the raw data of the input, output, and error signal, for one participant during one trial in terms of position, velocity, and acceleration control respectively.

The RMSE is computed for each trial, where e_i is the i th entry in the $N \times 1$ error vector e for each trial. N is the length of the input and the output signal ($N = 1900$).

It was inferred that participants learned the two *arctan* input functions over the progression of the experiment because their RMSE decreased. One-way ANOVA was performed to quantify intersubject and intrasubject variability [10]. Participants' performance error differed significantly across trials, such that $F_{7,1656} = 981.82$, $p < 0.05$. Intersubject variability was further quantified via multiple comparison analysis using the mean of the measured output, whereupon participants were classified into groups. Figure 3(a) shows a box plot of the participants' RMSE data across trials. The center line represents the median, the edges of the box are the 25th and 75th percentiles, the whiskers extend to the most extreme data points not considered outliers, and outliers are plotted individually. The Scheffe test, which uses an F-ratio to test for a significant difference between any two treatment conditions, was then used to determine which participants had similar mean errors. Figure 3(b) shows that the participants were grouped into 3 categories based on their RMSE. Error Group 1 (EG1) was composed of participants 1 and 4, Error Group 2 (EG2) was composed of participants 6 and 7, and Error Group 3 (EG3) was composed of participants 2, 3, 5, and 8. The purpose of grouping participants by their mean error was to quantify the effect of performance error on ones' control policy. In addition, we wanted to determine how many participants were described by the population average (AVG). It is standard practice within behavior experiments to average the participant data, with the idea that the greater the number of participants the more likely the participants will be explained by the population average [10]. However, due to our small population size (eight participants), we quantify the number of participants that are explained by the population average by comparing the mean error of each of the three groups and the population average via the Scheffe test. The top plot in Figure 4 shows that EG2 is statistically similar to the population average, thus 25% of the participants' performance error is described by the population average. The bottom plot in Figure 4 shows the RMSE across trials for each of the three groups and the population average. Within this view it



(a) Normalized RMSE of all subjects.



(b) Normalized RMSE of each learning group.

Fig. 3: Boxplots displays intersubject variability of normalized RMSE between all subjects and learning groups.

is qualitatively clear that the mean of group AVG is similar to the mean of group EG2. The only difference between groups AVG and EG2 is the empirical variance.

C. Subspace Identification

Subspace identification methods were used to generate models without prior specification of dynamic order. We considered a discrete time, linear, and time-invariant state space description of a dynamical system, given by

$$\mathbf{x}_{k+1} = \mathbf{A}\mathbf{x}_k + \mathbf{B}\mathbf{r}_k + \mathbf{w}_k \quad (2)$$

$$\mathbf{y}_k = \mathbf{C}\mathbf{x}_k + \mathbf{D}\mathbf{r}_k + \mathbf{v}_k, \quad (3)$$

for $k = 0, 1, \dots, N - 1$. Here, $\mathbf{x} \in \mathbb{R}^{n \times 1}$ is the state vector, $\mathbf{r} \in \mathbb{R}^{m \times 1}$ is the input signal, $\mathbf{w} \in \mathbb{R}^{n \times 1}$ is the process noise, $\mathbf{y} \in \mathbb{R}^{p \times 1}$ is the output signal, and $\mathbf{v} \in \mathbb{R}^{p \times 1}$ is the additive measurement noise. The process noise and measurement noise are assumed to be Gaussian white noise processes. Closed-loop subspace identification via the N4SID method was used to identify the unknown matrices $\mathbf{A} \in \mathbb{R}^{n \times n}$, $\mathbf{B} \in \mathbb{R}^{n \times m}$, $\mathbf{C} \in \mathbb{R}^{p \times n}$, and $\mathbf{D} \in \mathbb{R}^{p \times m}$ and the state trajectory \mathbf{x} , using the input \mathbf{r} and output data \mathbf{y} . n , the dimension of the state space, is equal to the size of the maximum singular value matrix for the case when the model order is not fixed. p and m are equal to 1 because we are modeling a Single Input Single Output (SISO) system. We removed 125 data points at the start of each trial and 175 at the end of each trial in order to focus

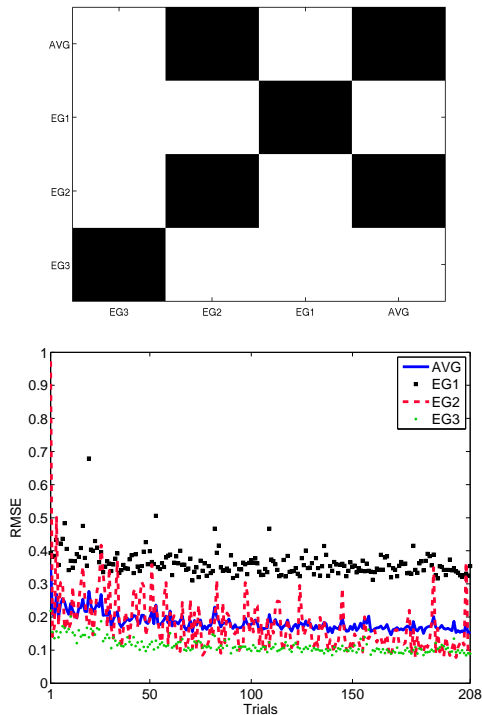


Fig. 4: Classification of participants via mean error. The top figure shows the multiple comparison analysis for each mean error group and the population average. The black indicates that the two comparisons are similar ($F\text{-ratio} < 4.07$) and the white indicates the two comparisons are different ($F\text{-ratio} > 4.07$). The bottom figure shows the RMSE per trial for the 3 groups: 2 participants for EG1, 2 participants for EG2, 4 participants for EG3.

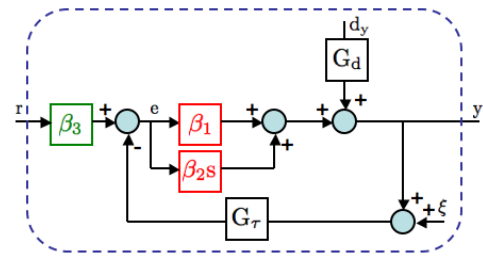
on the change in the signal. The delay of the sensorimotor system is accounted for in the subspace model by the fact that the output data points are delayed relative to the input data points. This delay was assumed to be a constant 150 ms. The MATLAB System Identification Toolbox was used to generate results. Further details of the algorithm are available in [14].

D. Relationship between PD and N4SID

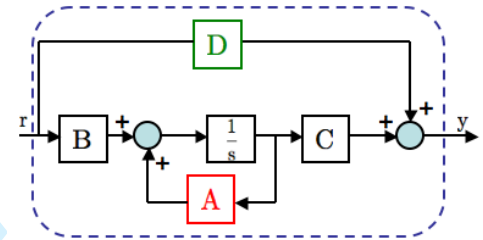
The three models that were chosen for comparison were a third-order proportional derivative controller, a third-order subspace model via N4SID, and a subspace model via N4SID where the model order is chosen based on the data. In a previous work [5], the motor behavior was described by a PD controller and a simple state space model was used to capture learning-related changes of feedback and feedforward control parameters across trials.

Figures 5(a) and 5(b) show the block diagram model of the PD controller model in terms of the frequency domain and a state space representation, respectively. In both diagrams, the overall model within the blue dotted line represents the human, including the cognitive internal model, which we associate with the controller and the body internal model, which we associate with the plant. The input r and output y were obtained in terms of voltage from the measurement

system. The green block denotes the feedforward information and the red block denotes the feedback information. G_d is a lowpass filter with transfer function $G_d = \frac{\phi}{s^2 + \gamma s + \phi}$, and $G_\tau = e^{-s\tau} \approx \frac{\frac{\tau}{12}s^2 - \frac{\tau}{2}s + 1}{\frac{\tau}{12}s^2 + \frac{\tau}{2}s + 1}$ is the second-order Padé approximation to account for the psychological motor delay of approximately 150ms. A lowpass filter is applied to the internal disturbance signal to correct for disturbances d_y that occur at lower frequencies [18]. For this particular system, the disturbance signal is attributed to reduced attention, plant (musculoskeletal) fatigue or random body movement. The error is denoted by e , and noise attributed to the experimental setup and visual feedback is denoted by ξ . The complementary



(a) PD Control Policy (closed-loop).



(b) Subspace Identification Control Policy (closed-loop) in basic state space form.

Fig. 5: Block-diagram models of the brain-body for both PD and subspace identification systems.

transfer function for the PD model is

$$T = \frac{Y(s)}{R(s)} = \frac{\beta_2 \beta_3 s + \beta_1 \beta_3}{\beta_2 G_\tau s + 1 - \beta_1 G_\tau}. \quad (4)$$

The subspace identification model generates parameters as state matrices (\mathbf{A} , \mathbf{B} , \mathbf{C} , \mathbf{D}). In order to compare the PD and subspace models, equivalent input-output realizations are compared. The poles of the PD models' complementary transfer function were compared to the eigenvalues of the \mathbf{A} matrix of the subspace model. For a first-order Padé approximation, this yielded $\lambda = \det(s\mathbf{I} - \mathbf{A}) = \frac{1 + \beta_1}{\beta_2} + \frac{2}{\tau}$. For a second-order Padé approximation or higher, we numerically solved for the eigenvalues. λ represents both the poles of the transfer function and the eigenvalues of the \mathbf{A} matrix. The pre-filter term β_3 of the PD model was compared to the \mathbf{D} matrix of the subspace model; $\mathbf{D} = \beta_3$. Henceforth, \mathbf{D} will not be written in boldface as we are dealing with a SISO system and it is scalar. The steady state gain (K) was calculated for both models and compared; $K = \lim_{s \rightarrow 0} \mathbf{C}(s\mathbf{I} - \mathbf{A})^{-1} \mathbf{B} + \mathbf{D} = \frac{\beta_1 \beta_3}{1 - \beta_1}$. The parameters β_i can be written in terms of the state space

parameters, where

$$\beta_1 = \frac{K}{D + K}, \quad (5)$$

$$\beta_2 = \frac{1 + \beta_1}{\lambda - \frac{2}{\tau}}, \quad (6)$$

$$\beta_3 = D \quad (7)$$

for a first-order Padé approximation. Again, for a second-order Padé approximation or higher, each β_2 is numerically calculated, where λ is each eigenvalue. Therefore the number of β_2 values depend on the number of eigenvalues.

III. RESULTS

A. Model validation and performance

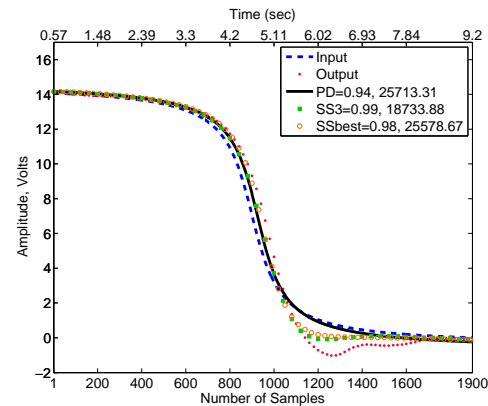
Spectral analysis was performed to verify accuracy of the three models and to investigate frequency related dynamics of the data for each group, in terms of signal position. Coherence and bandwidth were the most relevant spectral analysis metrics because they provided a direct interpretation of participants' physical movements. Coherence is used to measure the fraction of power in the output that can be attributed by a linear relationship from the input. Values of coherence range from 0 to 1; 0 indicating that the output and the input are completely unrelated, and 1 indicating that all the output is due to the input. To filter out noise and understand how coherence changed across trials, coherence measures were averaged across frequencies up to the bandwidth for each trial. The bandwidth was determined by finding the intersection of the gain crossover frequency for the complementary transfer function and the sensitivity transfer function [12].

In the experiment we found that as signal output decreased across trials, coherence increased. The relationship between signal output and coherence across trials revealed that participants initially produced more power than the input signal and decreased their power over trials in order to match the input signal. Change-point analysis was then used to determine at which trial significant changes in the coherence occurred [13]. Change-point analysis iteratively uses a combination of cumulative sum charts and bootstrapping to detect changes; it also provides a confidence level indicating the likelihood that a change occurred and a confidence interval indicating when the change occurred. Change-point analysis on the coherence data for each group showed the following significant increases in data ($p < 0.05$): changes for AVG occurred at trials 26, 66, 118, 158, 161, 165; changes for EG1 occurred at trials 23, 110; changes for EG2 occurred at trials 1, 58, 128; and changes for EG3 occurred at trials 26, 87, 158, 190. The results of the change-point analysis imply that participants who exhibit low error make more attempts at decreasing their signal power than other participants. Change-point analysis revealed that the bandwidth remained at a constant average of 0.65 Hz across trials for all groups, implying that all participants maintain the same range of movement frequencies across trials.

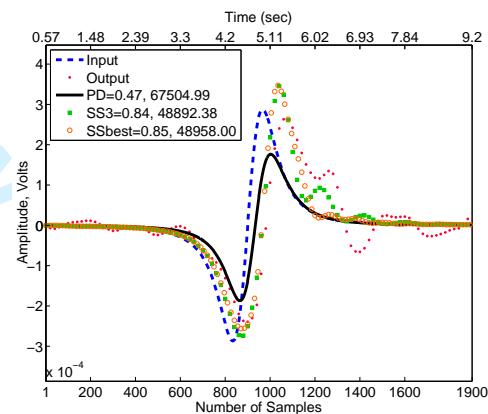
MATLAB was used to generate both PD and N4SID model estimates for data obtained in the experiment mentioned in Section II. Even trials were designated for model validation and odd trials were used for model development. Models were

constructed in terms of signal position and acceleration. In a previous work, Wohl [17] showed their visuomotor tracking model parameters were more sensitive to input changes in terms of acceleration despite ample practice. Given the simplicity of the \arctan input signal, we also investigated both position and acceleration as model input, in order to test their sensitivity for characterizing both learning and performance.

The Akaike Information Criteria (AIC) [19] and the coefficient of determination (R^2) [11] were calculated to provide a measured of how well future outcomes are likely to be predicted by the models. The AIC is a standard criteria used to



(a) Model results for signal position input signal.



(b) Model results for signal acceleration input signal.

Fig. 6: Comparison of the three algorithms for a given input corresponding for a trial (trial 30), where the first number indicates the R^2 value and the second number indicates the AIC value.

compare model performance for models with differing parameter size. Instead of measuring the direct distance between the predicted model output and the measured output, AIC measures an estimate of the distance. AIC is calculated by $-2\log(\mathcal{L}(\hat{\theta}|model, \mathbf{r})) + 2K$, where $\hat{\theta}$ are the estimated model parameters, model represents the SS3, SSbest, or PD models, \mathbf{r} is the input, and K is the number of estimated model parameters. The first term is the maximum log likelihood, which is the best fitting curve of the considered model. The second term is a penalty for over-fitting by increasing the number of parameters. The model with the smallest AIC is chosen as the model that best represents human response

behavior. Similarly, R^2 is a metric used to predict future outcomes on the basis of other related information, such as validation data. However, R^2 does not penalize models with larger parameter size and thus could give an inflated predicted fit for larger order models. Despite this deficiency, R^2 was calculated to confirm the AIC results as well as provide a range for how well the models perform on a scale from 0 to 1. Figures 6(a) and 6(b) show the predicted system response for a single trial of the three models for the AVG group in terms of signal position and acceleration, respectively. For both position and acceleration, the AIC and R^2 metrics reveal that the SS3 and SSbest models predict similarly well and better than the PD model.

Figure 7 shows AIC and R^2 results across trials for the four groups. The left column shows results for signal position, and the right column shows results for the signal acceleration. Both AIC and R^2 metrics show that all three models perform reasonably well for position and acceleration signal inputs. In addition, for all groups, signal inputs, and metrics, the SS3 model was best at predicting human performance followed by SSbest and PD. Change-point analysis was performed to determine which trials the models significantly ($p < 0.05$) over or under predicted the output. Changes are denoted by the bold square in figure 7. Change-point analysis revealed that more significant changes in prediction occurred for the signal input in terms of acceleration than position. This result is expected because each computed derivative of the performance input and output produces signals with smaller amplitude and larger variability. The greater the variability of the input and output signals the models are less able to predict performance, thus resulting in performance fluctuations as well as higher AIC and lower R^2 overall values. We further looked at the slope of the AIC and R^2 metric in order to determine how quickly models accurately predict human performance and how error influences the models' ability to predict human performance. The slope was obtained by performing a linear regression on the AIC and R^2 values across trials for all models, groups, and input signal types. The slopes of the R^2 metric for all models and groups that were constructed from the acceleration input signal were significantly greater (paired t-test: $p < 0.05$) than the corresponding R^2 slopes that were constructed from the position input signal. The slopes of the AIC metric for all models and groups that were constructed from the acceleration input signal were slightly greater (paired t-test: $p < 0.19$) to the corresponding AIC slopes that were constructed from the position input signal.

These results indicate that models constructed from signal acceleration have more learning related information. Results described in terms of acceleration capture more subtle nuances of control than position, thus capturing greater changes in learning. Change-point analysis confirmed that models constructed from signal acceleration are more sensitive than those constructed from signal position. The signal acceleration input produced models that exhibited substantial and consistent improvement in predicting performance, whereas models constructed from the signal position predicted performance with little change in accuracy over trials. A gradual improvement in the models' ability to accurately predict performance across

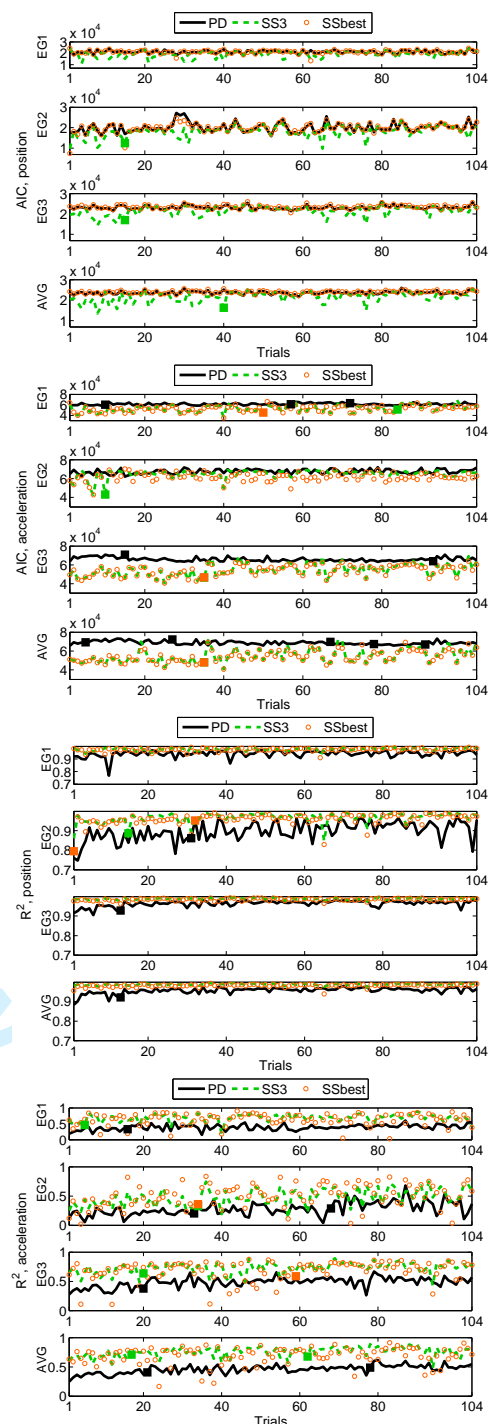


Fig. 7: AIC and R^2 values across trials for both signal position and acceleration for the three models for each learning group. AIC and R^2 results are in agreement, for signal position and acceleration the SS3 and SSbest models predicted similarly well and better than the PD model.

trials is important in order to display learning. Henceforth, we will only show results for models with the signal acceleration input because the focus of the paper is to describe model parameters in the context of both human performance and learning. Despite the fact that the models constructed from signal position produce more accurate predictions ($R^2 = 0.75 -$

0.99), models constructed from signal acceleration ($R^2 = 0.04 - 0.91$ where $R^2 > 0.20, 0.30, 0.40, 0.50$ for 96%, 89%, 78%, 62% of models respectively) produce reasonable predictions that are valid for observing human performance.

Poulton [20] showed that poor trackers have a large constant position error and a large variable error, whereas good trackers have a small constant position error and a small variable error. The variable error reflects the spread of the error distribution. However, connections between variable error, mean error, and model performance remain open. We find that large variability of error decreases the models' ability to predict performance. Moreover, models constructed from large variable error result in poorer prediction performance than models constructed from large mean error. The variable error and mean position RMSE for each group was quantified, such that [EG1, EG2, EG3, AVG] = [0.0385, 0.0920, 0.0223, 0.0270] for variable error and [0.3616, 0.1756, 0.1145, 0.1839] for mean RMSE. The mean AIC/R^2 and AIC/R^2 slope were quantified for each model for each group. EG2 had the largest variable error, similar mean RMSE to EG1 and AVG, the lowest mean AIC/R^2 values, and the greatest AIC/R^2 slope. EG2 had greatest improvement in performance over trials because the variable error decreased substantially over trials. However, EG1 had the largest mean RMSE but similar values for variable error, mean AIC/R^2 , and AIC/R^2 slope with EG3 and AVG. This shows that the variable error is a good indicator of model performance.

B. Feedback

In each of our models, the parameters that describe feedback are β_1 , β_2 , and the poles of the system transfer function or the eigenvalues of the \mathbf{A} matrix. In subsection II-D, β_1 and β_2 were defined as feedback parameters corresponding to the structure of the PD model and calculated in terms of the state space parameters. β_1 represents feedback in terms of position control and β_2 represents feedback in terms of velocity. The poles of the system transfer function represent the entire system feedback. The PD and SS3 models have three system poles, and the SSbest model has three or four system poles depending on the trial.

The mean and slope of the three feedback parameter were calculated in order to determine the evolution of parameters across trials. The slope was obtained by performing a linear regression on the β_1 and β_2 parameters, and the real part of the poles of the system transfer function, for all models and groups. The mean of β_1 , β_2 , the real part of the system poles across trials, for all models, and groups were 0.5, 1.5, and 0.9 respectively. The slope of β_1 , β_2 , the real part of the system poles across trials, for all models, and groups were 0.0002, 0.0002, and -0.0001 respectively. The imaginary parts of the system poles were analyzed in terms of variable error. The variable error of the imaginary part of one of the system poles (eig2) for SS3 and SSbest was significantly ($p < 0.05$) greater than the other system poles for all groups. Such that the variable error of eig2 for PD, SS3, and SSbest was 0, 0.032, 0.04 and the variable error of the other system poles for PD, SS3, and SSbest was 0, 0.016, 0.016. In addition, variable

error was calculated for every 10 trials for each system pole to determine if there was a trend in terms of how variable error changed over time. For all models and groups, there was no significant change in the variable error for each system pole over time.

From a control perspective, having the pole close to the unit circle suggests that the model (human performance) is slow to respond to changes. However, from the vantage point of modeling human performance we expect the system poles to be near the unit circle because human control has inherent delays. We expected that both the real and imaginary components of the system poles would decrease as performance improved across trials. However, no significant trends in feedback parameters across trials were found. The SS3 and SSbest models had imaginary components whereas the PD model did not. System poles without complex components define exponentially decaying components in the system response, whereas system poles with (stable) complex components generate a (decaying) sinusoidal response. The output in Figures 6(a) and 6(b) resemble decaying sinusoidal behavior, thus imaginary components of the system poles may be intrinsic to enhanced modeling of human motor control.

C. Feedforward

Since the feedback components remain constant throughout the experiment, the primary reason for improved participant performance can be presumed to be a feedforward mechanism. The D term is the parameter in the state space formulation that directly relates the input to the output. The state space formulation of $\mathbf{x}_{k+1} = \mathbf{A}\mathbf{x}_k + \mathbf{B}\mathbf{r}_k + \mathbf{w}_k$, $\mathbf{y}_k = \mathbf{C}\mathbf{x}_k + \mathbf{D}\mathbf{r}_k + \mathbf{v}_k$ shows that the relationship between the input \mathbf{r} and the output \mathbf{y} of the system is the parameter D. Because D is a scalar it was found equivalent to the β_3 parameter in the PD model as shown in subsection II-D. However for the case of multiple inputs and outputs, D will be a matrix where each entry within the matrix relates each input to each respective output.

From a physical standpoint, D is the amount of information that directly and instantaneously contributes to the output performance. Thus, it represents the knowledge of performing the task. We define learning as the change in the knowledge of performing the task. Knowledge of performing the task refers to an acquisition of both skill and strategy, for example through experience participants' understand how much force they need to apply to the knob or when and for how long they should apply the force. We perform linear regression on D over trials to quantify the amount of learning via the slope. Figure 8 shows D plotted across trials. Change-point analysis was performed to detect where significant changes occurred over trials. Changes are denoted by the bold squares. EG1 did not show any significant changes in D across trials. This is expected due to the high mean error. EG2 showed a significant change in D beginning at trial 65 and 84 for the PD and SS3 models respectively. EG3 showed a significant change in D beginning as early as trial 15 for the PD model and trial 21 for the SS3 model. AVG showed the combined effects of the previous 3 plots.

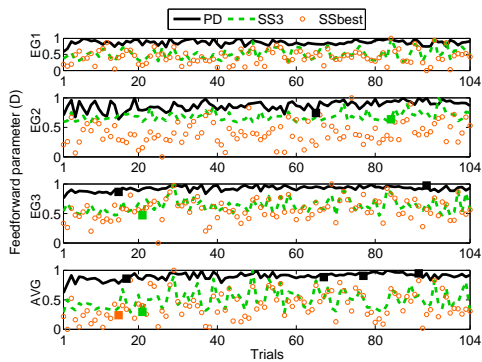


Fig. 8: D , the knowledge of performing the task, across trials for the three models for each learning group. Change-point analysis revealed that participants' (EG3) with the lowest mean error learned faster than other participants, whereas participants' (EG1) with the highest mean error did not show any significant changes in D .

Thus we can infer that participants with the lowest mean error learned faster than other participants. However, D did not capture learning trends for participants with mean error equal to or greater than EG1. The slope for each model for all learning groups was calculated. The slope for all models and groups EG2, EG3, and AVG were statistically similar, although the SS3 and SSbest models had a larger slope than the PD model. Thus, participants in groups EG2, EG3, and AVG learned the same. These results show that by adding an additional preprocessing step of separating participants by their mean error, we can extract more information from model parameters, such as how performance error effects learning. It is meaningful to be able to quantify how participants learn over time because that is the first step in systematically developing new ways to predict and improve ones' ability to learn. One additional point to mention is that D for individual trials represents only a snapshot of the feedforward information. Each snapshot does not tell us how much learning influences the next snapshot. Thus, D displays only incremental learning over time and does not reveal the accumulated learning or learning mechanisms operating across multiple trials.

D. Evolution of the policy over trials

As mentioned earlier, one of the unique advantages of the N4SID algorithm is that the model order can be predicted directly from the data. Thus, we can determine the complexity of participants' control policy over time. If the model order is unknown for the N4SID algorithm, the number of most significant singular values in one of the matrices describing the mapping from the input to the output will determine the model order. Figure 9 shows how the predicted model order varied over trials for each group. Each bar was obtained by summing the number of predicted third and fourth-order models for every 10 trials. The 11th bar only contains 4 trials, but it is scaled to reflect 10 trials so it is comparable with the other 10 bars. 71%, 72%, and 65% of the 104 trials resulted in third-order models for groups EG1, EG3, and AVG, respectively and 84% of the 104 trials resulted in fourth-order models

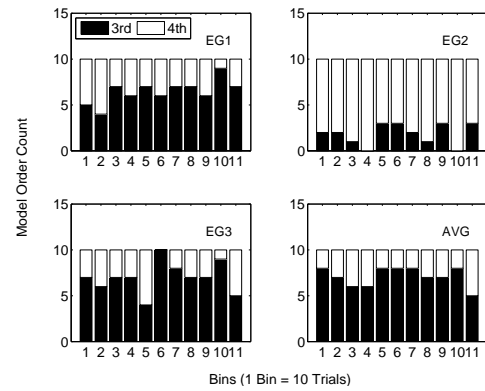


Fig. 9: The predicted model order distribution across trials for each learning group. The distribution reflects the evolution of the participants' control policy over time. Participants with the larger variable error (EG2) produced higher order models. For the particular input signal, the most suitable control policy to describe participant behavior resulted in a third-order model.

for group EG2. EG2 resulted in fourth-order models instead of third-order models because of the large variability in the error data. EG1 had the greatest mean error and EG2 had the greatest variable error. Larger variability in error leads to a higher order model despite mean error. Large fluctuations in the error signal will be included in the model because they appear to be important additional system dynamics. However, in our case the variability is part of the system itself, thus a higher order model is the most appropriate choice to capture the dynamics. In addition, for all groups, as error variability decreases over time, the model order approaches third-order.

IV. DISCUSSION

The main contribution of this paper is to develop a framework for how to interpret performance and learning for a human control model in the state space form. The framework consists of identifying feedforward and feedback state space parameters, evaluating the models' ability to predict the output for each trial, and performing an additional preprocessing step to reduce internal noise by grouping participants by their mean error.

We use three models as examples to demonstrate how to select the most appropriate model that best describes human motor performance and learning based on the framework. The three models that were chosen for comparison were a third-order proportional derivative controller, a third-order subspace model via N4SID, and a subspace model via N4SID where the model order is chosen based on the data. We hypothesized that the N4SID subspace identification model will be able to better predict the output of a given input signal than the PD model because N4SID offers a very flexible model structure. In agreement with our hypothesis, for all learning groups, signal inputs, and metrics the SS3 model was best at predicting human performance, followed closely by SSbest and PD. The results show that the SS3 model predicted the data slightly better than SSbest model because the SSbest model was trading-off performance to account for variability

in the data. We hypothesized that models constructed from the position input signal will have excellent performance but little learning-related information due to their initial accuracy, whereas models constructed from the acceleration input signal will show average performance and substantial learning-related information. AIC and R^2 metrics showed that all three models perform similarly well for position and acceleration signal inputs. In agreement with our hypothesis, the signal acceleration input produced models that exhibited substantial and consistent improvement in predicting performance, whereas models constructed from the signal position predicted performance with little change in accuracy over trials.

We have developed new metrics for quantifying performance and learning across trials using state space model parameters. We compared the PD and subspace model parameters, by solving for each one in terms of the other. We propose that learning-related changes describing feedforward can be directly described by parameters of the controller model, and learning-related changes describing feedback can be described by changes in feedback parameters. We focused our attention on the poles of the transfer function (eigenvalues in state space) and the steady state gain (D in state space) because it is well known that the state space realization can have infinitely many realizations. Characterizing system behavior in terms the eigenvalues and D is sufficient because the state space models are in terms of their minimal realization, thus the concern of parameter cancelation is avoided. In addition, we showed that the eigenvalues and D exhibit expected system related dynamics. For example, the eigenvalues were found to be near the unit circle with both real and imaginary components which correspond to sensorimotor delays and movement, respectively. D showed statistically significant increases over trials, corresponding to learning. The bandwidth and coherence results revealed the method of how participants improved their performance. Spectral analysis results showed that participants did not physically alter the speed of their hand movements to improve performance, but they acquired skills and strategies about how and when to apply force to the knob.

We showed how model performance, feedback, and feedforward parameters are influenced by both the mean and variance of the error. In agreement with system identification theory, we found that large variability between the input and output signals decreased the models' ability to predict performance. However, this finding is insightful because we have a quantitative marker for how much variance we can allow in our data and still produce reliable models. The results in this manuscript suggest that using input-output data with a variable error of approximately 0.4 or lower will lead to reasonably predictive models. The feedback parameters did not show any significant trends across trials for any of the learning groups. The feedforward component showed that participants with the lowest mean error learned faster than other participants. However, participants with the largest mean error did not show any significant changes in the feedforward component.

With the use of unstructured models, we confirmed that the evolution of the human control policy is dependent on the variability of the data. The larger the variability between the

input-output data the greater the number of model parameters needed to describe behavior. In the context of our experiment, we found that participants' variable error decreased over trials thus participants will adopt a lower order model over time.

In motor learning experiments, it is standard procedure to acknowledge individual subject differences and average the participants to bolster a reliable dataset. We showed that averaging participant performance statistically represented only 25% of the population, therefore we argue that classification of participants is necessary to accurately describe performance for small population groups.

ACKNOWLEDGEMENT

This research is supported by the Institute of Collaborative Biotechnologies (ICB) at the University of California Santa Barbara through grant DAAD19-03-D-0004 from the U.S. Army Research Office and P.H.S. grant NS44393. The authors are very grateful for the support from the NSF IGERT program and thank Jörn Diedrichsen and anonymous reviewers for their suggestions.

REFERENCES

- [1] R. Schmidt and T. Lee, *Motor control and learning: a behavioral emphasis*. Human Kinetics, 2005.
- [2] R. Klein and H. Jex, "Effects of alcohol on a critical tracking task," *J. of Studies on Alcohol*, vol. 36, pp. 11–20, January 1975.
- [3] R. Allen, A. Stein, and H. Jex, "Detecting human operator impairment with a psychomotor task," *JPL Publication*, vol. 81-95, pp. 611–625, October 1981.
- [4] S. Cheng and P. Sabes, "Modeling sensorimotor learning with linear dynamical systems," *Neural Comput.*, vol. 18, pp. 760–793, April 2006.
- [5] S. Grafton, P. Schmitt, J. Van Horn, and J. Diedrichsen, "Neural substrates of visuomotor learning based on improved feedback control and prediction," *NeuroImage*, vol. 39, pp. 1383–1395, February 2008.
- [6] E. Todorov and M. Jordan, "Optimal feedback control as a theory of motor coordination," *Nat. Neurosci.*, vol. 5, pp. 1226–1235, November 2002.
- [7] M. Sherback and R. D'Andrea, "Visuomotor optimality and its utility in parameterization of response," *IEEE Trans. Biomed. Eng.*, vol. 55, pp. 1783–1791, July 2008.
- [8] F. V. M. Sherback and R. D'Andrea, "Slower visuomotor corrections with unchanged latency are consistent with optimal adaptation to increased endogenous noise in the elderly," *PLOS Comput. Biol.*, vol. 6, pp. 1–13, March 2010.
- [9] V. Ethier, D. Zee, and R. Shadmehr, "Spontaneous recovery of motor memory during saccade adaptation," *J. Neurophysiol.*, vol. 99, pp. 2577–2583, March 2008.
- [10] F. Gravetter and L. Wallnau, *Statistics for the Behavioral Sciences*. Thomson Wadsworth, 7th ed., 2007.
- [11] N. Draper and H. Smith, *Applied Regression Analysis*. Wiley-Interscience, 1998.
- [12] J. Bendat and A. Piersol, *Random Data: Analysis and Measurement Procedures*. Wiley-Interscience, 3rd ed., 2000.
- [13] W. Taylor, "Change-point analysis: A powerful new tool for detecting changes," 2000.
- [14] L. Ljung, *System Identification: Theory for the User*. Prentice Hall PTR, 2nd ed., 1999.
- [15] H. Palanthandalam-Madapusi, S. Lacy, J. Hoagg, and D. Bernstein, "Subspace-based identification for linear and nonlinear systems," (Portland, OR, USA), pp. 2320–2334, ACC, June 2005.
- [16] Q. Xiong, A. Jiang, and A. Jutan, "Experimental investigation of subspace identification and lq control of a pressure tank," *ISA Transactions*, vol. 41, pp. 203–213, October 2002.
- [17] J. Wohl, "Man-machine steering dynamics," *Human Factors*, vol. 3, pp. 222–228, 1961.
- [18] S. Skogestad and I. Postlethwaite, *Multivariable Feedback Control Analysis and Design*. Wiley-Interscience, 2nd ed., November 2007.

- 1
2
3
4
5
6
7
8
9
10
11
12
13
14
15
16
17
18
19
20
21
22
23
24
25
26
27
28
29
30
31
32
33
34
35
36
37
38
39
40
41
42
43
44
45
46
47
48
49
50
51
52
53
54
55
56
57
58
59
60
- [19] K. Burnham and D. Anderson, *Model Selection and Multimodel Inference A Practical Information-Theoretic Approach*. Springer, 2nd ed., 2002.
- [20] E. Poulton, *Tracking Skill and Manual Controls*. New York: Academic Press, 1974.
- [21] R. Jagacinski and J. Flach, *Control Theory for Humans: Quantitative Approaches to Modeling Performance*. Lawrence Erlbaum Associates, 2003.
- [22] H. Akaike, "A new look at the statistical model identification," *IEEE Trans. Automat. Contr.*, vol. 19, pp. 716–723, December 1974.
- [23] D. Bauer, "Estimating linear dynamical systems using subspace methods," *Econometric Theory*, vol. 21, pp. 181–211, February 2005.
- [24] P. Van den Bosch and A. Van der Klauw, *Modeling, identification and simulation of dynamical systems*. CRC Press, Inc, 1994.
- [25] W. Bryan and N. Harter, "Studies in the physiology and psychology of telegraphic language," *Psychol. Rev.*, vol. 4, pp. 27–53, January 1897.
- [26] W. Bryan and N. Harter, "Studies on the telegraphic language, the acquisition of a hierarchy of habits," *Psychol. Rev.*, vol. 6, pp. 345–375, July 1899.
- [27] A. Chiuso and G. Picci, "Some algorithmic aspects of subspace identification with inputs," *Int. J. Ap. Math. Comput. Sci.*, vol. 11, no. 1, pp. 55–75, 2001.
- [28] I. Chou and S. Lisberger, "The role of the frontal pursuit area in learning in smooth pursuit eye movements," *J. Neurosci.*, vol. 24, pp. 4124–4133, April 2004.
- [29] J. Diedrichsen, Y. Hashamvohy, T. Rane, and R. Shadmehr, "Neural correlates of reach errors," *J. Neurosci.*, vol. 25, pp. 9919–9931, October 2005.
- [30] P. Fitts, "Perceptual-motor skill learning," vol. Categories of Human Learning, (New York), pp. 243–285, AW Melton, Academic Press, 1964.
- [31] A. Fuchs, "The progression-regression hypothesis in perceptual-motor skill learning," *J. Exp. Psychol.*, vol. 63, pp. 177–182, February 1962.
- [32] W. Garvey, "A comparison of the effects of training and secondary tasks on tracking behavior," *J. Ap. Psychol.*, vol. 44, pp. 370–375, December 1960.
- [33] B. Huang, S. Ding, and S. Joe Qin, "Closed-loop subspace identification: an orthogonal projection approach," *J. Process Contr.*, vol. 15, pp. 53–66, February 2005.
- [34] M. Jansson and B. Wahlberg, "A linear regression approach to state-space subspace system identification," *Signal Process.*, vol. 52, pp. 103–129, July 1996.
- [35] M. Jansson, "A new subspace identification method for open and closed loop data," vol. 16, IFAC World Congress, online, 2005.
- [36] R. Kalman, "A new approach to linear filtering and prediction problems," in *Journal of Basic Engineering*, vol. 82 of *D*, pp. 35–45, ASME, 1960.
- [37] T. Katayama, H. Kawauchi, and G. Picci, "Subspace identification of closed loop systems by the orthogonal decomposition method," *Automatica*, vol. 41, pp. 863–872, May 2005.
- [38] S. Lakshminarayanan, G. Emoto, S. Ebara, K. Tomida, and S. Shah, "Closed loop identification and control loop reconfiguration: an industrial case study," *J. Process Contr.*, vol. 11, pp. 587–599, October 2001.
- [39] L. Ljung and T. McKelvey, "Subspace identification from closed loop data," *Signal Process.*, vol. 52, pp. 209–216, July 1996.
- [40] R. Shadmehr and S. Wise, *The computational neurobiology of reaching and pointing*. The MIT Press, January 2005.
- [41] M. Smith and R. Shadmehr, "Intact ability to learn internal models of arm dynamics in huntington's disease but not cerebellar degeneration," *J. Neurophysiol.*, vol. 93, pp. 2809–2821, May 2005.
- [42] P. Van Overschee and B. De Moor, "A unifying theorem for three subspace system identification algorithms," *Automatica*, vol. 31, pp. 1853–1864, December 1995.



Jamilah A. Abdur-Rahim (Student Member, IEEE) received her B.S. in Electrical Engineering from Binghamton University State University of New York in 2003.

She is currently a Ph.D candidate in the Mechanical Engineering Department at the University of California, Santa Barbara, CA. Her research interests are in the areas of nonlinear dynamics and controls with applications in motor learning, system identification, and computational neuroscience.



Linda R. Petzold received her B.S. in Mathematics/Computer science from the University of Illinois at Urbana-Champaign (UIUC) in 1974, and the Ph.D. degree in Computer Science from UIUC in 1978. She was a member of the Applied Mathematics Group at Sandia National Laboratories, Livermore, California from 1978 to 1985. From 1985 to 1991, she served as Group Leader of the Numerical Mathematics Group at Lawrence Livermore National Laboratory. From 1991 to 1997, she was a Professor in the Department of Computer Science at the University of Minnesota. She is a member of the US National Academy of Engineering, and a Fellow of AAAS, ASME, and SIAM. She was awarded the Wilkinson Prize for Numerical Software in 1991, the Dahlquist Prize in 1999, and the AWM/SIAM Sonia Kovalevski Prize in 2003. She is the author of 2 books and over 150 journal articles.

Currently, she is a Professor in both the Department of Mechanical Engineering and Computer Science at the University of California, Santa Barbara. Her research interests are in the area of computational science and engineering, specifically in the areas of discrete stochastic simulation, multi-scale simulation, sensitivity analysis, and model reduction with application to systems biology and engineering.



Scott T. Grafton received his B.A. in Mathematics and Psychobiology from the University of California at Santa Cruz and his MD degree from the University of Southern California. After receiving his Ph.D, he was a research fellow in Neuroimaging at UCLA where he developed methods for mapping human brain activity using positron emission tomography, and held appointments at University of Southern California; Emory University; and Dartmouth College (director of the Brain Imaging Center). He is action editor for the journal *NeuroImage* and is on the editorial board of *Annals of Neurology*, *Clinical Neurophysiology*, *Experimental Brain Research* and the *Journal of Cognitive Neuroscience*. He is a member of the Board of Scientific Counselors of the NIH intramural branch and has served as an NIH study section member. He is the author of over 115 journal articles.

Currently, he is a professor in the Department of Psychology at the University of California, Santa Barbara (UCSB) and is director of the UCSB Imaging Center since 2006. His research interests are in the areas of motor learning and control of goal oriented action, with particular emphasis on uncovering the cognitive architecture that underlies action representation.



Francis J. Doyle III (Fellow, IEEE) received his B.S. from Princeton University in 1985, C.P.G.S. from Cambridge in 1986, and Ph.D. from Caltech in 1991, all in Chemical Engineering. After receiving his Ph.D, he was a Visiting Scientist at DuPont in the Strategic Process Technology Group, and held appointments at Purdue University; the University of Delaware; and the Universität Stuttgart. He is the recipient of several research awards including: National Science Foundation National Young Investigator; Office of Naval Research Young Investigator; Alexander von Humboldt Research Fellowship (2001-2002); and AICHE CAST Division Computing in Chemical Engineering Award (2005). He is the author of 3 books, and over 150 journal articles.

Currently, he is a professor in the Department of Chemical Engineering at the University of California, Santa Barbara and has been the Suzanne and Duncan Mellichamp Endowed Chair in Process Control since 2002. His research interests are in the areas of systems biology and nonlinear process control, with applications ranging from gene regulatory networks to complex particulate process systems.